

1
2
3
4
5 **RUT INITIATION MECHANISMS IN ASPHALT MIXTURES AS GENERATED UNDER**
6
7 **ACCELERATED PAVEMENT TESTING**
8

9
10 **Salil Gokhale¹, Bouzid Choubane², Tom Byron² & Mang Tia³**
11

12
13 ⁽¹⁾ Applied Research Associates, Inc., ERES Consultants Division,
14 5007 N.E. 39th Avenue, Gainesville, FL 32609
15 Phone: (352) 955-6312
16 Fax: (352) 955-6345
17 E-mail: sgokhale@ara.com
18

19 ⁽²⁾ Florida Dept. of Transportation, Materials Research Park
20 5007 N.E. 39th Avenue, Gainesville, FL 32609
21 Phone: (352) 955-6302, Fax: (352) 955-6345
22 E-mail: bouzid.choubane@dot.state.fl.us
23 E-mail: tom.byron@dot.state.fl.us
24

25 ⁽³⁾ University of Florida
26 Department of Civil and Coastal Engineering
27 Weil Hall, PO Box 116580
28 Gainesville, FL 32609
29 Phone: (352) 392-9537, Fax: (352) 392-3394
30 E-mail: tia@ce.ufl.edu
31

32
33
34 **Word Count:**

35 Body text = 3048
36 Abstract = 185
37 Tables 4 x 250 = 1000
38 Figures 9 x 250 = 2250
39 **Total Words = 6483**
40
41
42
43
44
45
46
47
48
49
50
51
52

ASBTRACT

The Florida Department of Transportation (FDOT) conducted an experiment to address the effects of polymer modifiers on the performance of Superpave mixes using a Heavy Vehicle Simulator (HVS). Two fine-graded Superpave mixes were considered. One mix included a virgin binder meeting the requirements of PG 67-22, while the other contained a SBS polymer-modified binder meeting those of PG 76-22. Both respective mixes contained the same effective binder content, aggregate components and gradation. The mixes were designed for 10-30 million ESALs, using the standard Superpave mix design methodology. During placement of these mixes, all standard FDOT density requirements and acceptance criteria were applicable.

The subsequent investigation showed that the sections with SBS-modified mixture significantly outperformed those with the unmodified mixture. It was also determined that rutting in the unmodified mixture was primarily a function of shear flow while rutting in the SBS-modified mixture was due mainly to densification.

This paper presents a description of the testing program, the data collection effort and the subsequent analyses and findings focusing primarily on the initiation mechanisms of rutting in asphalt mixtures as generated and observed under accelerated pavement testing.

INTRODUCTION

Permanent deformation or rutting is characterized by a longitudinal depression that forms in the wheel paths. This form of distress occurs in flexible pavements due to the accumulation of small permanent deformation in any of the pavement layers or the subgrade. Such deformations may be caused by too much repeated stress being applied to the pavement layers or (and) by an asphalt mixture that is too low in shear strength. In the first case, the rutting is considered more of a structural or construction problem. It is generally the result of an underdesigned or undercompacted pavement section, or of a subgrade that has been weakened by the intrusion of moisture. In the second case, the rutting is normally a mixture related problem. When an asphalt pavement layer has inadequate shear strength, a small, but permanent, shear deformation occurs each time a heavy truck applies a load. A rut will then appear with enough load applications. This distress type reduces pavement serviceability and poses a safety hazard.

BACKGROUND

The need for faster and more practical evaluation methods under closely simulated in-service conditions prompted the Florida Department of Transportation (FDOT) to consider Accelerated Pavement Testing (APT). APT is generally defined as the controlled application of realistic wheel loading to a pavement system simulating long-term, in-service loading conditions. This allows the monitoring of a pavement system's performance and response to accumulation of damage within a much shorter time frame. APT can produce early, reliable and beneficial results while improving pavement technology and understanding/prediction of pavement systems performance.

Florida's APT Facility

Florida's Accelerated Pavement Testing and Research program is housed within the new State Materials Research Park in Gainesville. The testing site consists of eight linear test tracks with each test track measuring approximately 45 m (150 ft long) by 3.6-m (12 ft wide). Two additional test tracks were designed with water-table control capabilities within the supporting base and subgrade layers. The accelerated loading is performed using a Heavy Vehicle Simulator (HVS), Mark IV model. The HVS is electrically powered (using external electric power source or electricity from an on-board diesel generator), fully automated, and mobile. The HVS functionality has recently been enhanced to include automated laser profiling and test track temperature control capabilities.

Initial Experiment

The first experiment in Florida's APT program was designed to address the effects of polymer modifiers on the performance of fine-graded Superpave mixes with a 12.5 mm nominal aggregate size. One mix included a virgin binder meeting the requirements of PG 67-22, while the other contained a polymer-modified binder meeting those of PG 76-22. These mixes contained the same effective binder content, aggregate components and gradation, details of which are shown in Table 1. The mixes were designed for 10-30 million ESALs, using the standard Superpave mix design methodology. This required that all volumetric properties, aggregate consensus properties, and moisture susceptibility meet the Superpave criteria.

The respective Superpave mixes were placed in two, 50 mm (2 in) lifts to construct seven distinct test tracks (or lanes) while complying with all the standard FDOT construction, materials, in-place (as

constructed) specifications and methods. The supporting layers consist of a 265 mm (10.5 in) limerock base over a 305 mm (12 in) limerock stabilized subgrade. During placement of all these layers (both asphalt and supporting layers), all standard FDOT density requirements and acceptance criteria were applicable. All the asphalt layers, for instance, were compacted to 93 ± 1 percent of the maximum specific gravity. A substantial array of thermocouples was placed during construction to allow for temperature monitoring at the asphalt/base interface and at a 50 mm (2 in) depth in the asphalt. Test track surface thermocouples were mounted after construction. For the initial experiment, five test tracks (numbered 1 through 5) were considered, with each track subsequently divided into three replicate testing sections (referred to herein as sections A, B, and C) for a total of 15 possible test sections. The intent of these three replicate sections within each track was to allow for a statistically sound experiment design. Test tracks 1 and 2 were constructed using two layers of polymer modified asphalt mixture, track 3 was constructed using one layer of polymer modified mix over one layer unmodified mix, while tracks 4 and 5 were constructed using two layers of unmodified asphalt mix, as shown in Figure 1. The remaining two test tracks (6 and 7) were tested for the purposes of a separate study, and, therefore, were not considered in this paper. The load was applied on all test sections through a Goodyear G165 (305 mm wide) super-single tire loaded to 40 kN (9000 lbs) at a speed of 12 km/h (8 mph). The load was applied in a unidirectional mode with a 100 mm (4 in) wheel wander, in 25 mm (1 in) increments, with the tire pressure maintained at approximately 790 kPa (115 psi) (1). The tests were conducted at a controlled temperature of 50° C, at a depth of 50 mm (2 in) using radiant heaters. In addition, two sections (1A and 2A) were tested at a higher temperature of 65° C. Automated longitudinal and transverse surveys of the resulting ruts were performed at predetermined intervals using a set of laser sensors.

In addition to accelerated load tests, a comprehensive laboratory testing program was also conducted to characterize both the mixtures and the liquid binders. The results of this test program are presented elsewhere (2).

OBJECTIVE

The primary objective of this study was to assess both the relative rut performance of the asphalt mixtures and the prevalent mechanisms actually involved in the subsequent rut formation.

DATA COLLECTION

Rut measurements were collected at predetermined intervals in the form of longitudinal and transverse profiles during the course of this study. These rutting profiles were collected after every 100 passes during the early phase of testing, and after every 1000 passes as the test progressed. The profiles were automatically acquired using a laser-based system installed on the HVS loading assembly/carriage. This profiling system consists of two lasers mounted 762 mm (30 in) apart on either side of the load carriage. The lasers, model SLS 5000™ manufactured by LMI Silicon, are specified to be accurate to within ± 0.2 percent of the measurement range.

At each predetermined number of load passes, the profile measurements were taken following a directional pattern as shown in Figure 2. In such a pattern, the lasers, while traveling with the “unloaded” carriage, surveyed an area of approximately 5.9 m (20 ft) in length and 1.70 m (5.5 ft) in width in a series of 67 fluid and continuous sweeps. The data was collected at a rate of 16 kHz and averaged at 100 mm (4 in) intervals. Following this process a total of 58 transverse profiles are generated, at any given number of load passes. The initial profile (profile after construction and before loading) was used as the reference

(baseline) to estimate the rut depths for the purpose of this study. A set of typical transverse profiles for a given test section is presented in Figure 3.

In addition to rut data, four to six core samples were also obtained from each test section, both before and after accelerated testing. The cores were taken along the longitudinal alignment within both the loaded (wheelpath), the “humped” (edges of wheelpath), and the unloaded areas (2). Furthermore, full-depth trench slabs were recovered from each of the three combinations of pavement sections for further forensic evaluation.

DATA ANALYSIS

Rutting Profiles

As described previously, 58 transverse profiles were generated for every test section, at any given number of passes. The rut depth was determined from each profile as the maximum distance between a straight line drawn from the two highest points on the humps (on each side of the wheelpath) and the lowest point on the wheelpath, as shown in Figure 4.

The different surface profiles, as plotted in Figure 3, illustrate the development of upheavals (humps) of asphalt concrete at the edges of the wheelpath and depressed areas in the wheelpath. All these deformations may be a result of the flow of materials towards the respective edges of the wheelpath and/or densification. If rutting were caused by densification alone, no humps would have formed at the edges of the wheelpath.

Identification of Densification and Shear

Changes in Layer Thickness and Air Void Content

A forensic (“post-mortem”) investigation of the three trench slabs revealed that all deformation in the test tracks were confined to the asphalt layers only. The layer thicknesses as obtained from these slabs are summarized in Table 2. As previously stated, the rutting in an asphalt layer usually occurs as a result of consolidation (densification) and/or lateral shoving (shear flow) of the asphalt materials under traffic loads. The densification induces a reduction of in-place air void content, whereas the shear flow may not necessarily be accompanied by a change in air void content. A one percent change in the volume of asphalt mixture can be related to a one percent change in its air void content. Assuming that volume change occurs in the vertical direction only, then a one percent change in the air void content of a layer should result in a one percent change in the height of that layer. On the other hand, if the in-place asphalt mixture densifies equally in all three directions, then a one percent reduction in its air void content would result in a change of 0.33 percent in its height. (3, 4)

Thickness of each core was measured at 4 points on the core, and averaged to obtain the mean core thickness. In addition, the air void content of each core was determined according to the procedure described in AASHTO T 166-93, *Bulk Specific Gravity of Bituminous Mixtures Using Saturated Surface Dry Specimens* (5). Average air void content and layer thickness measurements, before and after loading are summarized in Table 3. The cores recovered from the wheelpath show a reduction in both air void content and thickness, whereas the cores recovered from the edges of the wheelpath show an increase in air void content and thickness. An important point to note is that some variability is intrinsic to these measurements as cores cannot be recovered from the same exact location.

Furthermore, in order to investigate whether differential densification occurred in the two asphalt layers of a pavement, a second set of cores was obtained from the wheelpath, edge of the wheelpath (hump) and from the untrafficked areas from four test sections. These cores were split along the layer interface, and air void content and layer thickness were then measured for each layer. Percent changes in the layer thickness and air void content were calculated for each core and are presented in Figures 5 and 6. A solid line drawn in both figures indicates a 1:1 ratio (equality line) between layer thickness changes and change in air void content. If densification in the vertical direction were solely responsible for rutting, then all the points would fall on the equality line. If densification occurred in all three directions, then these data points should fall above the equality line, and if shear flow as well as densification occurred, then the points should fall below the equality line (3, 4). Figure 5 shows that most of the data points fall below the line of equality. This indicates that most of the layers had a greater reduction in thickness than densification alone could have induced. This figure also does not show any significant direct relationship between respective changes in void contents and layer thicknesses. Therefore, shear flow must be responsible for the movement of material out of the wheelpath and into the outer sides of the wheelpath. In addition, as can be seen in Figure 6, core samples from the top layer exhibited an increase in thickness and air void content, whereas cores from the bottom layer exhibited reduction in thickness and air void content.

Changes in Wheelpath and Hump Volume

Another method of determining the amount of rutting caused by shear flow is to examine the proportional relationship between the accumulated volume of material at the edge of the wheelpath (humps) and the volume of displaced material within the wheelpath. For analysis purposes, one could reasonably assume that, at constant total volume, if the material at the edge of the wheelpath (humps) has been displaced from the wheelpath solely by shear flow, then the corresponding ratio of the volume of the “humps” to the volume of the empty space in the wheelpath can be attributable to shear flow. The remaining part would, thus, be attributable to densification (3, 4). A hump to wheelpath volume ratio of 1.0 would therefore indicate that shear flow is fully responsible for the rut development.

Using such an approach, the transverse profiles collected during this study were analyzed to determine the respective volumes at the edge of the wheelpath and within the wheelpath. As described earlier, each set of data consisted of 58 transverse profiles, which were averaged to develop a representative transverse profile for a given number of HVS passes. This representative profile was then superimposed on the original (untrafficked) profile of that particular test section. The areas at the edge of the wheelpath (hump) and the area of the void space within the wheelpath, illustrated in Figure 7, were determined by numerical integration. The respective volumes were then determined by multiplying these areas by a unit length of 1 meter. This process was repeated for every single surface profile generated during the course of this study. A series of ‘macros’ were written in Visual Basic for Applications (VBA) to automate the acquisition of the raw laser data as well as to perform the necessary calculations. A large amount of data was therefore analyzed to determine the ratio of volume of the “hump” to the volume of the void space in the wheelpath. A summary of this analysis is presented in Table 4.

Generally, it is believed that rutting is initially caused by densification i.e., reduction of level of air voids, in the wheelpath, and later due to the shear flow of the asphalt concrete. The hump to wheelpath volume ratio was plotted against the number of HVS wheel passes for every test section. Figures 8 and 9 illustrate the progression of the hump to wheelpath volume ratio as determined during this study. Two distinct trends can be observed in these two figures. For unmodified asphalt mixtures, the hump to wheelpath volume ratio sequentially increases with increasing number of HVS passes, whereas, for modified asphalt mixtures this ratio seems to remain approximately constant. It can also be noted that for test sections 3A and 3B (with one layer of modified asphalt and one layer of unmodified asphalt mix), the

1
2
3 trend in the hump to wheelpath volume ratio agrees closely to that of the test sections made with two
4 layers of modified asphalt mix. Previous studies concluded that at high tire pressures, higher
5 temperatures increase the proportion of shear flow as compared to the proportion of densification, for
6 comparable test sections (3, 4). As described previously, in this study, sections 1A and 2A were tested at
7 65° C, to evaluate rutting at higher temperatures. Although the magnitude of rutting was considerably
8 higher, the proportion of rutting attributable to shear flow was not significantly different than comparable
9 test sections at 50° C.

10 11 12 **RESULTS AND DISCUSSION**

13
14
15 Analysis of rutting data indicates that the unmodified asphalt concrete mixtures rutted significantly more
16 than the modified mixtures under similar loading and temperature conditions. The rate of rut
17 development is also significantly higher in the unmodified mixtures.

18
19 The densification-shear analysis produced some interesting results. It was expected that, at the beginning
20 of the test, densification would be the major factor in rut development, as the initial level of air voids
21 would decrease in the wheelpath due to repeated wheel loads. However, looking at Figures 8 and 9, it can
22 be seen that even after only 100 passes, approximately 40-50 percent of rutting can be attributable to
23 shear flow. That is, volume of the asphalt concrete in the humps is approximately half the volume of the
24 wheelpath. This indicates that rutting may be caused simultaneously by densification and shear flow of
25 the asphalt concrete. Figure 8 also shows that, for unmodified asphalt mixtures, the ratio of hump to
26 wheelpath volume increases with increasing number of HVS wheel passes. This indicates that, after an
27 initial number of wheel passes, a majority of the rutting occurs only because of shear flow. In
28 comparison, for the modified asphalt mixtures, however, the ratio of hump to wheelpath volume remains
29 somewhat constant, with approximately 40 percent of rutting caused by shear flow.

30
31 An important factor to be noted is that during the course of this study, there was no permanent
32 deformation within of the limerock base layer as all the rutting was confined to the asphalt layers alone.
33 This stiff base layer may have affected the formation of humps at the edge of the wheelpath.

34
35 In conclusion, since the only variable between the two superpave mixes considered in this study is the
36 asphalt binder type, the rut initiation (or initiation mechanism) is primarily controlled by the stiffness of
37 the asphalt binder.
38
39
40
41
42
43
44
45
46
47
48
49
50
51
52

REFERENCES

1. Byron T., Choubane B., and M. Tia. *Assessing Different Loading Configurations in Accelerated Pavement Testing*, Proceedings of the 2nd International Conference on Accelerated Pavement Testing, Minneapolis, MN, September 2004, CD-ROM.
2. Sirin O., Kim H-J, Tia M., Choubane B. and T. Byron. *Evaluation of Rutting Resistance of Superpave Mixtures With and Without SBS Modification By Means of Accelerated Pavement Testing*, 2003 Annual Meeting of the Transportation Research Board, TRB/NAS, Washington D.C., #03-1226, CD-ROM, January, 2003.
3. Harvey J. and L. Popescu. Accelerated Pavement Testing of Rutting Performance of Two CALTRANS Overlay Strategies. In *Transportation Research Record: Journal of the Transportation Research Board, No. 1716*, TRB, National Research Council, Washington, D.C., 2000, pp. 116-125.
4. Harvey J. and L. Popescu. “*Rutting of CALTRANS Asphalt Concrete and Asphalt-Rubber Hot Mix Under Different Wheels, Tires, Temperatures – Accelerated Pavement Testing Evaluation*”. Draft Report prepared for California Department of Transportation, Pavement Research Center, CAL/APT Program, Institute of Transportation Studies, University of California, Berkeley, January 2000.
5. AASHTO T 166 – 93. Bulk Specific Gravity of Bituminous Mixtures Using Saturated Surface Dry Specimens. American Association of State and Highway Transport Officials, Part II – Tests.

LIST OF TABLES

TABLE 1 Mix Design and Volumetric Properties for Asphalt Mixes

TABLE 2 Layer Thicknesses Measured From Trench Slabs

TABLE 3 Average Core Air Void Content and Thickness Before and After HVS Testing

TABLE 4 Summary of Ratios of Hump/Wheelpath Volumes

LIST OF FIGURES

FIGURE 1 Pavement cross sections of different test tracks.

FIGURE 2 Path of laser profiler in measuring pavement surface profile.

FIGURE 3 Typical transverse profiles for Section-4A.

FIGURE 4 Schematic of measurement of rut depth.

FIGURE 5 Comparison of percent change in thickness to percent change in air void content, wheelpath cores.

FIGURE 6 Comparison of percent change in thickness to percent change in air void content, edge of wheelpath (hump) cores.

FIGURE 7 Schematic illustration of hump and wheelpath areas in a transverse profile,

FIGURE 8 Progression of hump To wheelpath volume ratio, unmodified mixtures.

FIGURE 9 Progression of hump to wheelpath volume ratio, modified mixtures.

TABLE 1 Mix Design and Volumetric Properties of Asphalt Mixtures

Percentage by Weight of Total Aggregate Passing Sieves							
Type Material	S-1-A Stone	S-1-B Stone	Screenings	Local Sand	JMF	Control Points	Restricted Zone
Blend	12%	25%	48%	15%			
Number	1	2	3	4			
Sieve Size	¾ in 19.0 mm	99	100	100	100	100	
	½ in 12.5 mm	45	100	100	100	93	90-100
	3/8 in 9.5mm	13	99	100	100	89	-90
	No.4 4.75mm	5	49	90	100	71	
	No. 8 2.36 mm	4	10	72	100	53	28-58
	No. 16 1.18mm	4	4	54	100	42	25.6-31.6
	No. 30 600µm	4	3	41	96	35	19.1-23.1
	No. 50 300µm	4	3	28	52	22	
	No. 100 150µm	3	2	14	10	9	
	No. 200 75µm	2.7	1.9	5.9	2.2	4.5	2-10
G _{sb}	2.327	2.337	2.299	2.546	2.346		
Volumetric Properties							
Mix Type	Asphalt Binder	% Binder	V _a @ N _{des}	VMA	VFA	P _{be}	G _{mm}
Virgin Mix (Compacted at 300° F)	PG 67-22	8.20	4.0	14.5	72	4.97	2.276
SBS-Modified Mix (Compacted at 325° F)	PG 76-22	7.90	3.8	14.2	73	4.90	2.273

TABLE 2 Layer Thickness Measured From Trench Slabs

Test Section	Average Thickness (mm)		
	Wheelpath	Edge of Wheelpath	Non-trafficked
2B-Top Layer (Modified)	35	39	39
2B-Bottom Layer (Modified)	37	41	41
3B-Top Layer (Modified)	36	40	39
3B-Bottom Layer (Unmodified)	39	40	40
4B-Top Layer (Unmodified)	42	50	46
4B-Bottom Layer (Unmodified)	33	39	38

TABLE 3 Average In-Place Air Void Content and Thickness, Before and After HVS Testing

Average Air Void Content (%)						
Test Section	Untrafficked		Inside Wheelpath		Edge of Wheelpath	
	Average	St. Dev	Average	St. Dev	Average	St. Dev
Both layers modified (6 test sections)	6.7	0.9	3.7	0.6	6.4	0.3
Top layer modified, Bottom layer unmodified (3 test sections)	7.7	0.1	5.0	1.0	7.5	0.3
Both layers unmodified (6 test sections)	7.0	0.5	4.8	0.9	8.7	1.1
Average Thickness (mm)						
Test Section	Untrafficked		Inside Wheelpath		Edge of Wheelpath	
	Average	St. Dev	Average	St. Dev	Average	St. Dev
Both layers modified (6 test sections)	88.3	7.6	84.9	8.3	90.3	8.1
Top layer modified, Bottom layer unmodified (3 test sections)	80.4	2.3	76.2	2.1	81.3	5.0
Both layers unmodified (6 test sections)	89.9	1.6	82.0	4.8	93.9	6.3

TABLE 4 Summary of Ratios of Hump/Wheelpath Volumes

Test Section Number	Test Temperature (°C)	Final Rut Depth (mm)	Final Number of HVS Passes	Volume Along 1-m Long Section (m ³) x 10 ⁻³		Percent of Rutting Attributable To:	
				Within Wheelpath	Edge of Wheelpath (Hump)	Shear	Densification
1A	65	12.5	130,000	2.80	1.22	44	56
1B	50	7.8	140,060	1.64	0.69	42	58
2A	65	11.7	160,000	2.77	0.92	33	67
2B	50	9.2	240,000	1.85	0.70	38	62
3A	50	11.3	275,000	2.51	1.11	44	56
3B	50	12.0	280,032	2.37	1.26	53	47
4A	50	16.5	95,478	2.72	2.33	86	14
4B	50	17.0	65,000	2.73	2.30	84	16
5A	50	15.6	113,945	3.20	1.74	54	46
5B	50	20.7	62,935	3.11	3.20	100	0

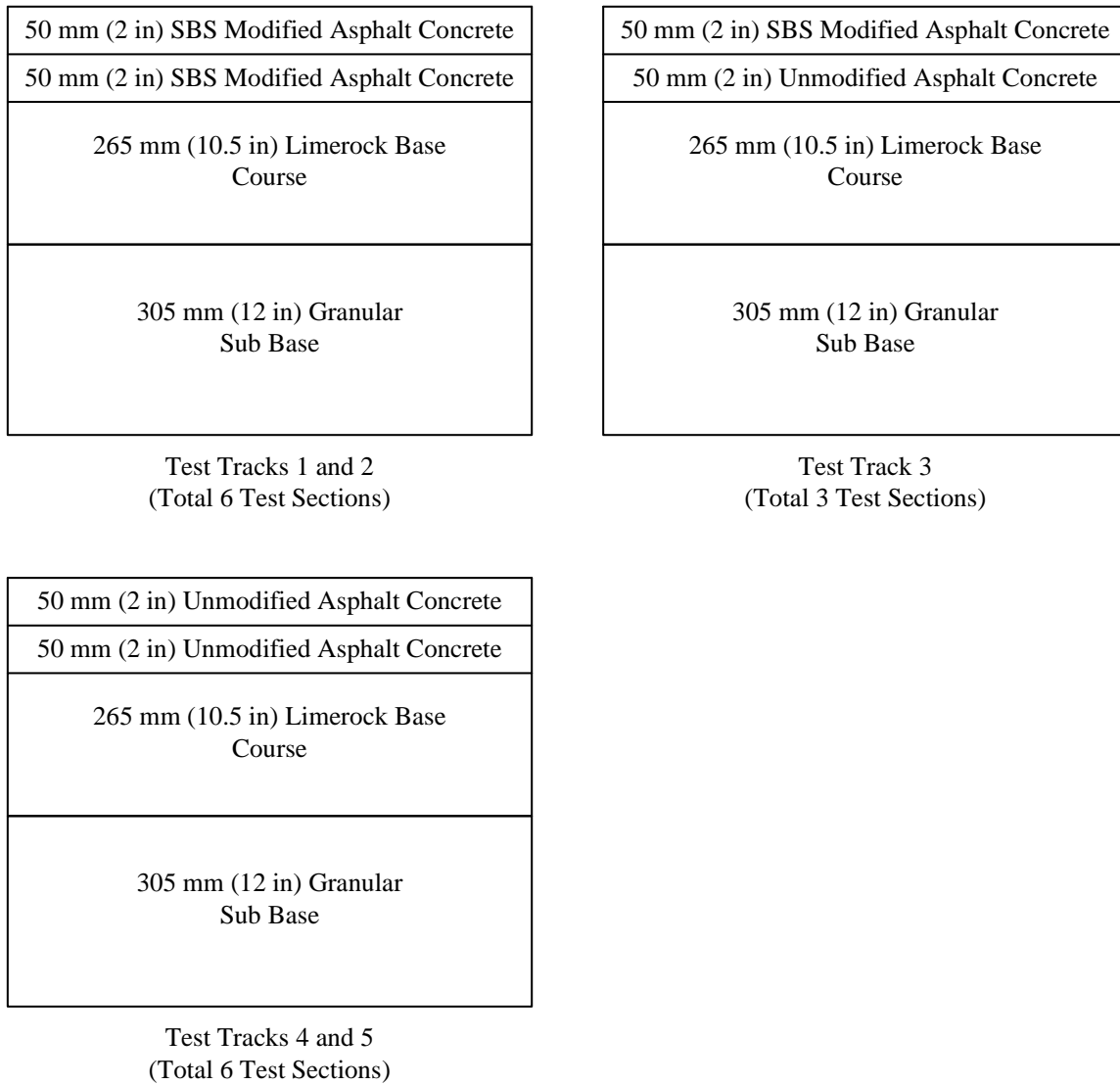


FIGURE 1. Pavement cross sections of different test tracks.

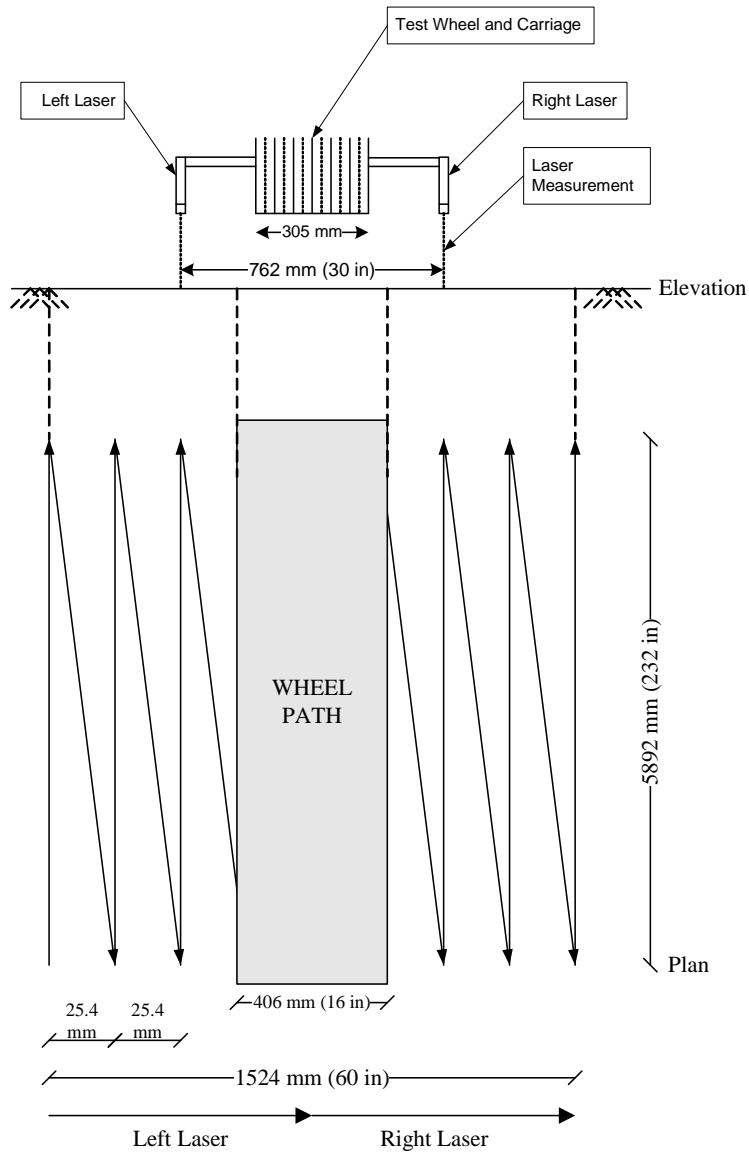


FIGURE 2 Path of laser profiler for measuring pavement surface profile.

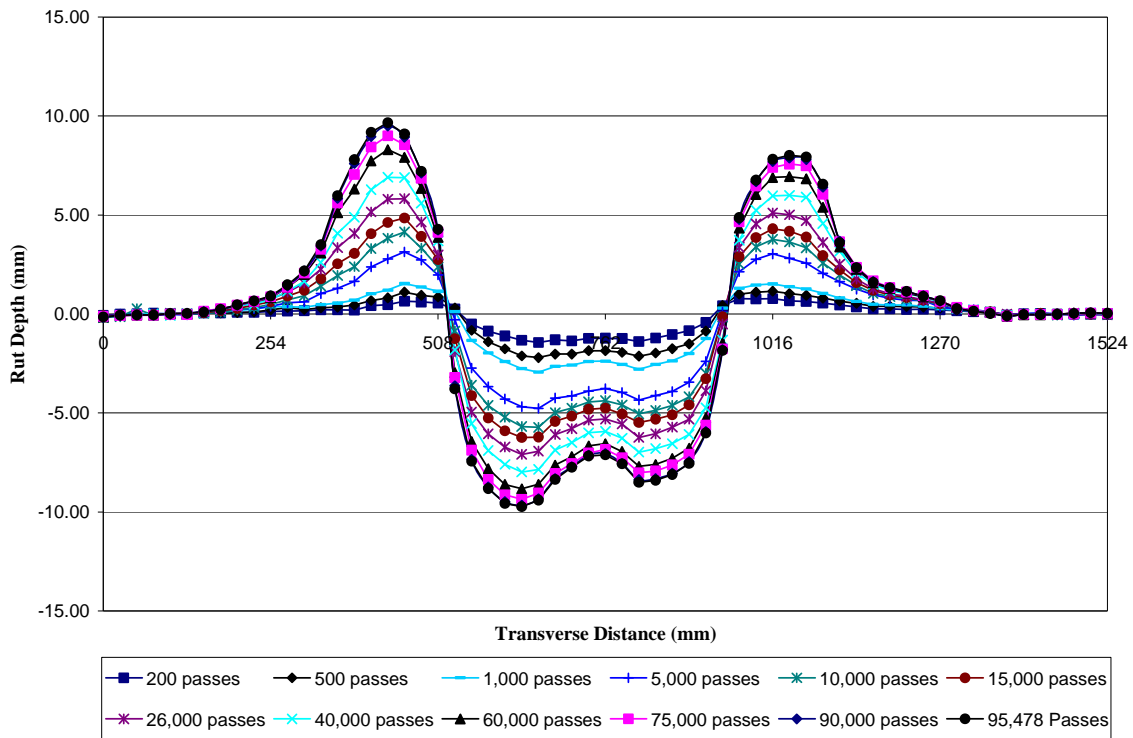


FIGURE 3 Typical transverse profiles for test Section-4A.

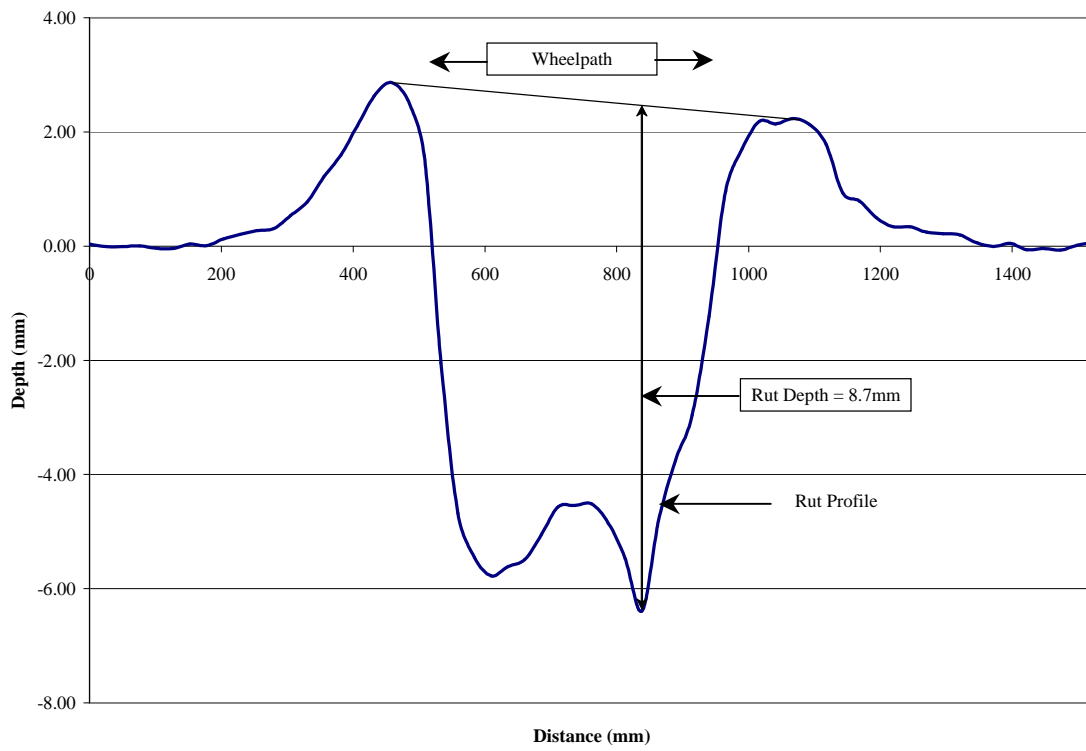


FIGURE 4 Schematic of measurement of rut depth.

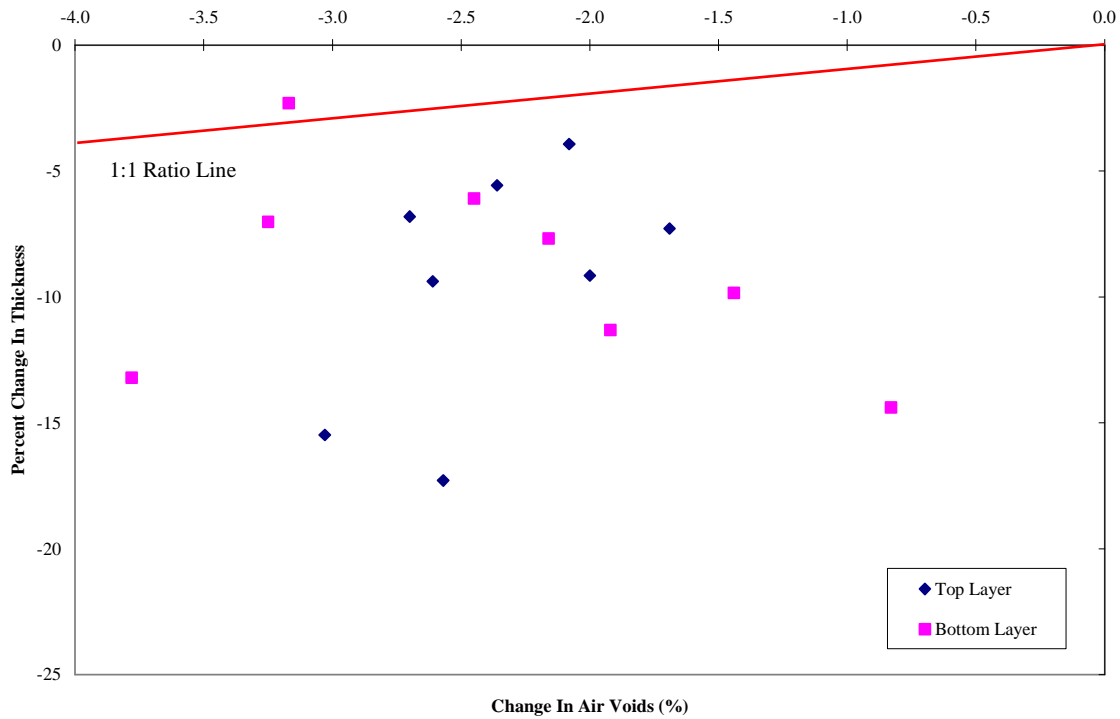


FIGURE 5 Comparison of percent change in layer thickness to percent change in air void content, wheelpath cores.

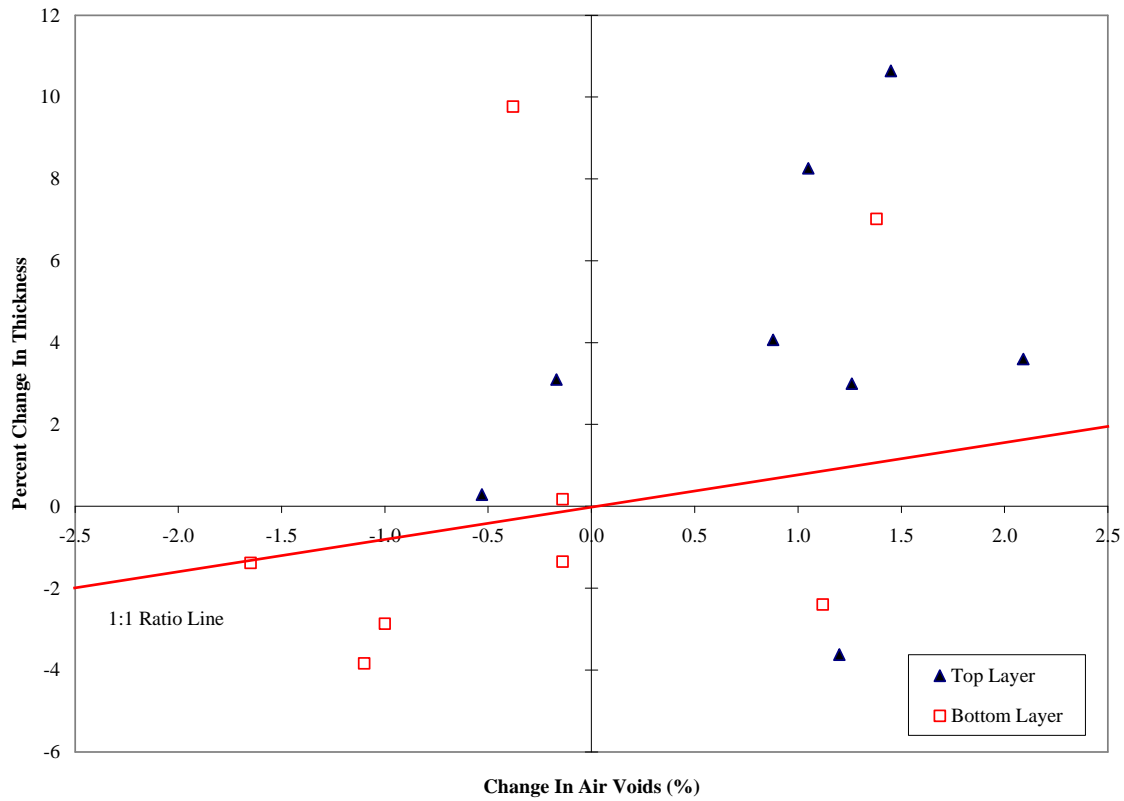
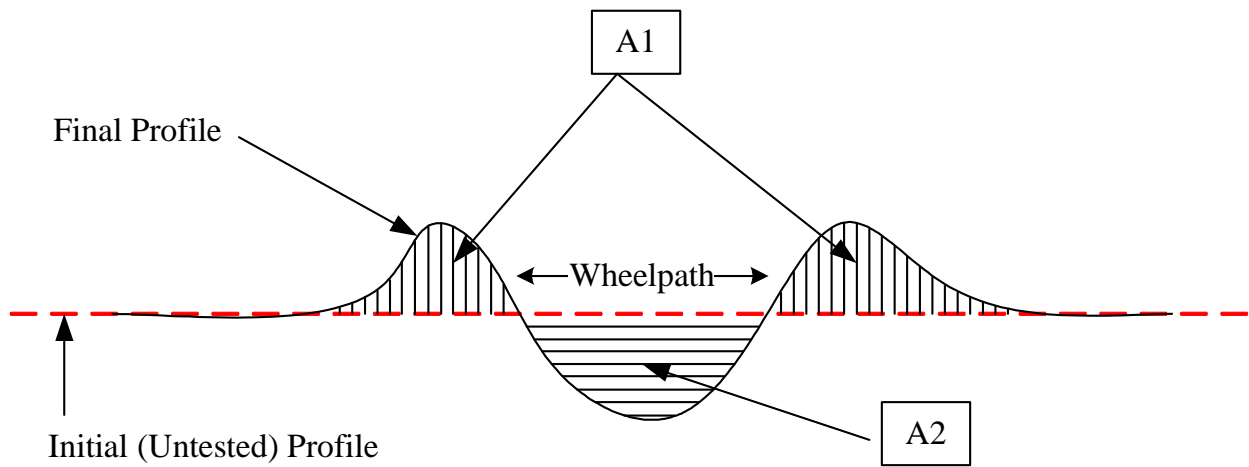


FIGURE 6 Comparison of percent change in layer thickness to percent change in air void content, edge of wheelpath (hump) cores.



A1 = Area of material at the edge of wheelpath (Humps)

A2 = Area of empty space inside the wheelpath

Figure 7 Schematic illustration of hump and wheelpath areas in a transverse profile.

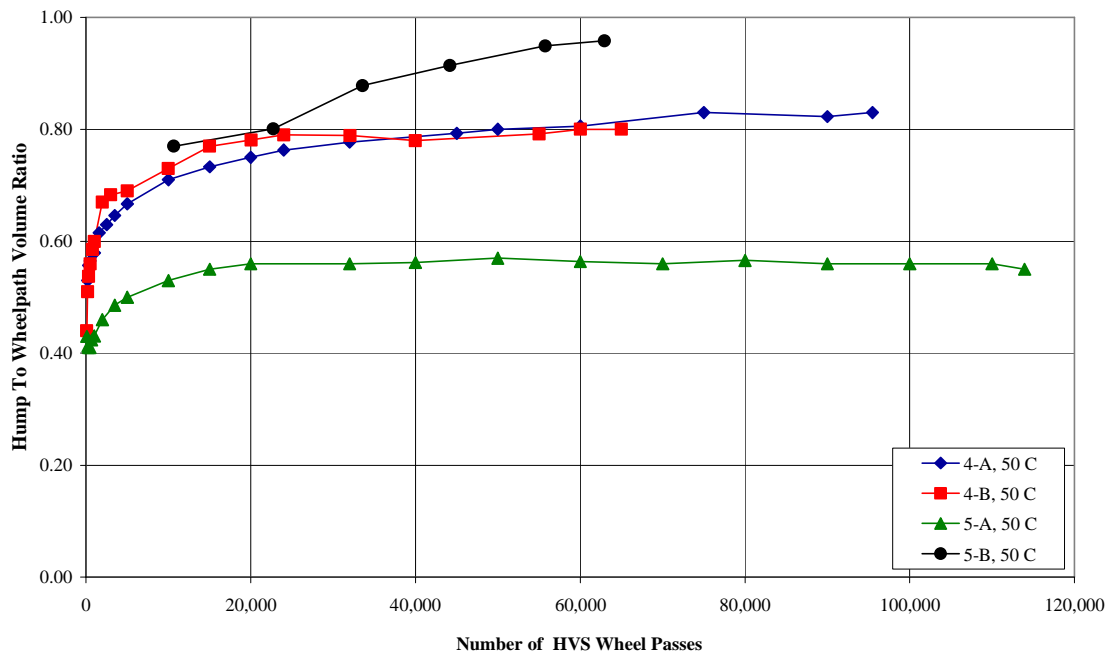


FIGURE 8 Progression of hump to wheelpath volume ratio, unmodified mixtures.

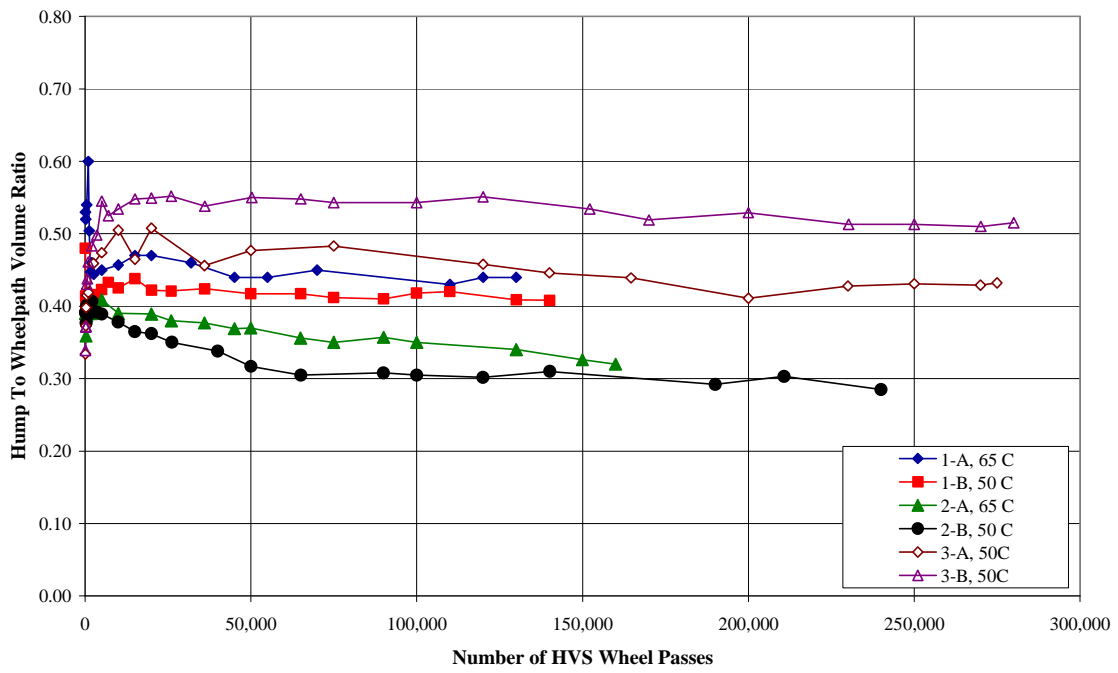


FIGURE 9 Progression of hump to wheelpath volume ratio, polymer modified mixtures.